Investigation on the performance characteristics of chloride selective electrode in concrete

Ming Jin[1] · Jinxia Xu[1] · Linhua Jiang[1] · Yi Xu[1] · Hongqiang Chu[1]

Abstract A monitoring technique based on the chloride selective electrodes for the chloride content in concrete which is accurate, non-destructive, and continuous would be highly desirable. For this reason, the performance, such as Nernst response and resisting polarization, of the electrode was tested both in simulated concrete pore solutions and concrete. Moreover, the surface morphology of electrode after immersion in solutions over 3 months was detected. Results revealed that the electrode potential showed a good Nernst response with chloride concentration and was affected little by sulfate ion. The detection limit for the chloride concentration was 10^{-3} mol L^{-1} at pH 13.5 and 10^{-4} at lower pH values. In addition, the electrode also had a high exchange current density and a high equivalent capacitance. The Ag/AgCl coating showed good long-term stability over 3 months in solutions containing chloride ions. Besides, there was a good agreement between the free chloride content determined by the electrode and by pore solution expression.

Introduction

Steel embedded in concrete is prevented against corrosion by a thin passive film that is formed on the steel surface due to the high alkaline environment of concrete [1]. However, corrosion of rebars due to chloride ions (Cl$^-$) from sea water or deicing salts is the main cause of damage and early failure of reinforced concrete structures [2]. The best way to avoid the corrosion-induced damage is prevention, including monitoring the aggressiveness of the environment [3]. It might be the ratio of chloride to hydroxide ions that is of more importance than the chloride content alone [4–6]. The threshold value of Cl$^-$/OH$^-$ determined in the simulated concrete pore solutions ranges from 0.25 to 1 where corrosion initiation is expected [6]. There have been efforts to develop methods for determining the Cl$^-$ concentration in concrete. And a lot of lab techniques and field measurements for measuring Cl$^-$ content in RC have been adopted. The most popular techniques are potentiometric and Volhard methods. They can detect both free and total chlorides in concrete cores extracted from in-service structures. However, these techniques are mostly destructive, time-consuming, and costly [7]. To make things worse, they cannot obtain the change of Cl$^-$ concentration in concrete pore solution.

Differing from these destructive methods, the non-destructive techniques (NDT) do not change the environment and the future usefulness of the concrete where the measurement is taken [2]. Moreover, these non-destructive monitoring techniques could be taken at several points and times, which will allow developing practical methods for determining and predicting structural lifetime and repair/maintenance scheduler [8–10]. The most studied and developed methods could be divided into the following: (i) electrical resistivity [11–13], (ii) optical fiber sensors [14–16], and (iii) ion selective electrodes (ISE) [2, 3, 17–20]. However, the electrical resistivity methods are very sensitive to the moisture content. And for most of electrical resistivity techniques, the surface must be wet because the conductivity is zero for dry concrete. In addition, the optical fiber sensors also have some drawbacks that are significant for reliable and accurate measurements. For example, optical fiber needs enough protection to stop its

✉ Linhua Jiang
lhjiang@hhu.edu.cn

[1] College of Mechanics and Materials, Hohai University, Nanjing 210098, People's Republic of China

break during casting or service life [21]. Furthermore, optical fiber sensors need additional protection to separate the fiber from corrosive environments.

However, the ISE shows good chemical stability in aggressive environments and the fabrication is easy through electrochemical processes. They can monitor the change of Cl⁻ concentration with time in concrete pore solution. The Ag/AgCl electrode is widely used and commercially available as chloride selective electrode. The commonly used way to manufacture the Ag/AgCl electrode was the electroplating method. However, it should be pointed out that the current density used by the literature [22] was too large to get the dense AgCl coating. We have reported that it was appropriate to apply the current density of 0.1 mA/cm² to anodize the electrode [23].The first attempt to use Ag/AgCl electrodes to measure the Cl⁻ concentration in cement-based materials was introduced by Atkinson et al. [17, 24]. They reported that Ag/AgCl electrodes could be used as in situ sensors for monitoring Cl⁻ concentration in the short-term (less than 3 months) tests in their experimental conditions. Elsener [2] found that the chloride sensors followed the Nernst law with good linearity in a range from 0.005 to 4 mol L⁻¹ Cl⁻ concentration and the Cl⁻ concentrations measured in situ by these sensors were in good quantitative agreement with that determined by pore solution squeezing. Montemor [3] reported that the effective chloride diffusivity estimated by the embedded Ag/AgCl electrodes in mortar specimens is about 2×10^{-12} m s⁻².

However, there are many factors that induce measurement errors and must be considered: interferential ions, temperature, alkalinity, and long-term life. Atkins [18] stated that temperature could lead to errors and the presence of bromide would give an overestimate of chloride concentration. The high alkalinity of solutions can result in an interference in potentiometric response of Ag/AgCl electrodes, especially at low chloride concentration [25]. The sensitivity of electrodes to chloride concentration was easily found in the literatures [3, 7, 25], but there was less reports about the sensitivity of electrodes to the value of [Cl⁻]/[OH⁻] which has been considered practical to predict the steel corrosion. What is more, there was also less literatures about the performance of electrodes of resisting polarization in alkaline solutions with and without chloride.

In this paper, the performance, such as Nernst response and resisting polarization, of the electrode was investigated both in simulated concrete pore solutions and concrete. And the surface morphology of electrode after immersion in solutions over 3 months was detected. In addition, the chloride concentrations determined by the electrodes were compared to data obtained from pore solution expression.

Theoretical background

The Ag/AgCl electrode

The Ag/AgCl electrode is a solid electrode which consists of a silver wire with a dense coating of silver chloride. The potential of the electrode, $E_{Ag/AgCl}$, follows Nernst's law:

$$E_{\mathrm{Ag/AgCl}} = E_{\mathrm{Ag/AgCl}}^{\mathrm{o}} - \frac{RT}{nF} \ln a_{\mathrm{Cl}^-} \tag{1}$$

Here, F is t−he Faraday constant, R is the gas constant, T is the absolute temperature (K), and a_{Cl^-} is the activity of the Cl⁻ in solution.

When it is at room temperature and $n = 1$, Eq. (1) becomes as follows:

$$E_{\mathrm{Ag/AgCl}} = E_o + 0.059 \cdot \log[Cl^-] \tag{2}$$

However, the term [Cl⁻] refers not to chloride concentration C_{Cl^-} but to the chloride activity a_{Cl^-} linked by the activity coefficient γ_{Cl^-}:

$$a_{Cl^-} = C_{Cl^-} \cdot \gamma_{Cl^-} \tag{3}$$

When testing in solutions containing chloride, the value of γ_{Cl^-} can be taken reasonably as $\gamma_{\mathrm{Cl}^-} = 1$ and thus, the chloride concentration can be determined directly from Eq. (3).

Interfering ions

Many ions such as OH⁻, Br⁻, and I⁻ can interfere the potential of Ag/AgCl electrode [18]. These interfering ions are commonly taken into account by use of selectivity coefficients, $k_{i,j}^{\mathrm{pot}}$ (i stands for the primary and j for the interfering ions). Thus, Eq. (1) is written in the following form, the so-called Nikolskij-Eiseman equation [26, 27]:

$$E_{\mathrm{Ag/AgCl}} = E_{\mathrm{Ag/AgCl}}^{\mathrm{o}} - \frac{RT}{nF} \ln \left(a_{\mathrm{Cl}^-} + \sum_j \left(k_{Cl^-,j}^{\mathrm{pot}} \cdot a_j^{-1/z_j} \right) \right) \tag{4}$$

Here, a_j is the activity of the interferent and z_j its charge.

The detection limit of the Ag/AgCl electrode varies with pH values. When the pH values range from 11.9 to 13.7, chloride concentrations below 2×10^{-4} to 7×10^{-3} mol L⁻¹ cannot be accurately detected by electrodes due to the OH⁻ interference. For this reason, the free Cl⁻ concentration being responsible for corrosion initiation of the steel can be adequately determined by the Ag/AgCl electrodes in the pore solutions of concrete.

Stability of AgCl coating at alkaline environment

It is necessary to investigate the stability of AgCl coating in alkaline environments; otherwise, the application in concrete pore solution is not feasible. In the presence of hydroxide ions, the AgCl coating can undergo metathesis and become partially covered with AgOH. This reaction only happens at sufficiently low chloride concentration, namely of the following condition is fulfilled:

$$\frac{K_s(\text{AgOH})}{K_s(\text{AgCl})} > \frac{a_{\text{OH}^-}}{a_{\text{Cl}^-}} \tag{5}$$

At 25 °C, $K_s(\text{AgCl})$ and $K_s(\text{AgOH})$ are 1.8×10^{-10} and 2×10^{-8}, respectively. Thus, when the hydroxide ion concentration is 100 times larger than the chloride concentration, the AgCl coating may transform into Ag_2O. The pH value of concrete pore solution usually lies between 12.5 and 13.5. So the AgOH might be formed when the chloride concentration is below 0.003 mol L^{-1} at pH 13.5 and below 0.0003 mol L^{-1} at pH 12.5. However, AgOH is unstable and tends to convert to Ag_2O. The electrode coating consisting of AgCl acts as a chloride ISE as discussed above, but the electrode coating with Ag_2O is sensitive to hydroxide ions and thus the electrode acts as a pH sensor rather than a chloride sensor. The $\text{Ag}/\text{Ag}_2\text{O}$ electrode potential also follows Nernst's law:

$$E_{\text{Ag}/\text{Ag}_2\text{O}} = E^o_{\text{Ag}/\text{Ag}_2\text{O}} - \frac{RT}{F} \ln a_{\text{OH}^-} \tag{6}$$

Here, the standard electrode potential, $E^o_{\text{Ag}/\text{Ag}_2\text{O}}$, can be estimated at ca. 345 mV vs. SHE from solubility product constants K_s at 25 °C of the reaction $\text{Ag}_2\text{O} + \text{H}_2\text{O} \leftrightarrow 2\text{Ag}^+ + 2\text{OH}^-$. In the case of complete transformation of the AgCl surface into Ag_2O, the electrode potential would be determined by Eq. (6) and assume the value $E_{\text{Ag}/\text{Ag}_2\text{O}}$ = 142 mV vs. SCE at pH 13.5, 190 mV vs. SCE at pH 12.5.

Experimental

Preparation of the Ag/AgCl electrode

These Ag/AgCl electrodes used in this paper were manufactured from 99.99 % pure silver wires (0.5 mm dia.). These wires were degreased with acetone; immersed in 5 % mass fraction nitric acid (HNO$_3$) for 10 min, and placed in anhydrous ethanol with ultrasonic vibration for 5 min. Then, the wires were anodized galvanostatically in 0.1 mol L^{-1} hydrochloric acid (HCl) for 1 h under a current density of 0.2 mA/cm^2. After anodizing, electrodes were kept in 1 mol L^{-1} Potassium chloride (KCl) out of direct sunlight until

used. The electrodes were connected electrically with a Cu wire and the junction was sealed with epoxy resin. The exposed area was about 0.0628 cm^2.

Tests in simulated concrete pore solutions

The pH value of a fresh concrete may vary in the range 13.5–12.5, approximately. Along with the carbonation process, the pH value of concrete pore solution drops; however, the pH value will not drop to 7. In our work, the aqueous solutions of pH ranging from 13.5 to 6.86 were used. The compositions and pH values of solutions are given in Table 1.

All reagents used in our work were of analytical grade. For the electrochemical measurements, the chloride electrode, the cylindrical platinum foil, and the saturated calomel electrode (SCE) were connected to serve as working electrode, counter electrode, and reference electrode, respectively. All the electrochemical tests were performed with a Princeton Applied Research (PAR) STAT 2273 Potentiostat. If not specified, all the tests were carried out at room temperature (25 °C) and exposed to laboratory air.

Nernst response of electrodes

Sensitivity to chloride ion The tests were performed three times in solutions A–E containing known concentrations of sodium chloride (NaCl) ranging from 10^{-5} to 1 mol L^{-1}. Apart from investigating the sensitivity of chloride sensors to chloride concentrations, the interference of alkalinity to the sensitivity of electrode was measured. Besides, the detection of electrodes to the value of [Cl$^-$].[OH$^-$] in these solutions was detected.

Sensitivity to sulfate ion Sulfuric acid usually exists in the external environment of concrete. Thus, it is necessary to investigate the effect of sulfuric acid on the potential of chloride electrodes. In our work, different amounts of sulfuric acid were added into the 3.5 % wt. NaCl solution. The sulfuric acid concentrations were 0.002, 0.006, 0.01, 0.05, 0.1, and 0.5 mol L^{-1}, respectively.

Effect of temperature Measurement curves were obtained at several temperatures as follows: 4, 15, 30, and 45 °C. The

Table 1　Composition and pH value of the solution used

Solution	Composition	pH value
A	8 g NaOH +35.6 g KOH per liter of saturated Ca(OH)$_2$ solution	13.5
B	Saturated Ca(OH)$_2$ Solution	12.5
C	0.025 M NaHCO$_3$ + 0.025 M Na$_2$CO$_3$	10
D	0.01 M Na$_2$B$_4$O$_7$	9.18
E	0.025 M mixed phosphate	6.86

response of the electrodes under alkaline environment was tested in the saturated Ca(OH)$_2$ solution (SCS) with NaCl concentrations ranging from 10^{-3} to 1 mol L^{-1}.

Polarization test of electrode

Potentiodynamic polarizations were performed in all solutions A–E without chloride and the solution A containing different NaCl concentrations. The scan rate was 0.2 mV/s and the potential sweeps went from −150 to 200 mV against the open-circuit potential (OCP). The same solutions were also used for electrochemical impedance spectroscopy (EIS) tests. The EIS tests were conducted in the frequency ranging from 100 kHz to 10 mHz. Tests were repeated for three times using different samples.

Galvanostatic tests were performed also in the SCS with different chloride concentrations. A cathodic direct current (DC) of 0.05 μA was applied to the chloride electrodes for 100 h. After this, the current was stopped, and the chloride electrodes were allowed to recover to their initial OCP.

Long-term stability

Chloride electrodes were immersed in solutions A, B, and D with two different chloride concentrations. The immersion period was over 3 months. The electrode potential was periodically tested versus a SCE in each solution. All solutions were sealed completely in order to avoid carbonation in atmosphere. After 3 months, some selected electrodes were examined with the scanning electron microscope (SEM) equipped with energy-dispersive spectrometers (EDS).

Tests in concrete

Cylindrical concrete samples 50 mm in diameter and 70 mm in length with a centrally embedded chloride electrode were cast with w/c 0.6. After curing for 3 weeks, the top and bottom faces of the samples were coated with epoxy resin. The diagram of the specimen is shown in Fig. 1. These specimens
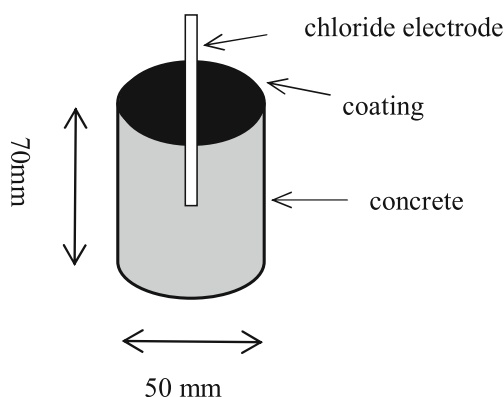

Fig. 1 Concrete specimen with chloride electrode embedded in the center

were then immersed in NaCl solutions (0, 0.1, 0.5, and 1 mol L^{-1}). Measurement of the potential of the embedded chloride electrode was performed versus a SCE placed in the solution. After a total immersion time of 1 year, pore solutions of concrete were expressed with a pressure of about 350 MPa. Chloride concentrations were subsequently analyzed in the expressed pore solutions by a volumetric technique.

Results and discussion

Tests in simulated concrete pore solution

Nernst response of electrode

Sensitivity to chloride ion Figure 2a shows the electrode potentials measured in solutions A–E with chloride concentration ranging from 10^{-5} to 1 mol L^{-1}. The results of the critical detection values and the slopes of the curves in different chloride concentrations are given in Table 2 for all five solutions. The potential remained unchanged when the chloride concentration was lower than 10^{-3} mol L^{-1} at pH 13.5. And the potential of Ag/AgCl electrode was almost same when the chloride concentration was less than 10^{-4} mol L^{-1} at lower pH values. Thus, the critical value of detecting chloride concentration at pH 13.5 was 10^{-3} mol L^{-1} but the critical value was 10^{-4} mol L^{-1} at other pH values. In addition, the slope of the theoretical curve is ca. 59 mV/decade (in Fig. 2a). But these measured curves have a little difference with the theoretical curve, which is ascribed to the mean activity coefficient and the liquid junction potential [25]. What is more, the Ag/AgCl electrode potential follows a linear relationship with the logarithm of chloride activity ranging from 10^{-3} to 1 mol L^{-1}. Figure 2b indicates the sensitivity of electrode potential to chloride concentration at pH 13.5; the selectivity coefficient can be calculated according to Eq. (4), which is approximately 6.8×10^{-4} and lower than the value reported in the literature [22]. Based on this value and the measured curves, the limit of chloride ion detection would be around 10^{-3} mol L^{-1} when the OH$^-$ concentration is 0.315 mol L^{-1} (pH = 13.5). What is more, when the chloride concentration is higher than 10^{-2} mol L^{-1}, the electrode potential has a good linear relationship with the chloride concentration and the slope is 51 mV/decade in this area (Fig. 2b), which is located in the "working region." However, the slope decreases to 35 mV/decade when the chloride concentration ranging from 10^{-2} to 10^{-3} mol L^{-1}, which is located in the "poor region." It will enter the "bad region" when the chloride concentration is lower than 10^{-3} mol L^{-1}, in which the electrode potential is no longer sensitive to chloride concentration; at this time, the potential remains unchanged. Figure 2c shows the electrode potential against the chloride concentration at pH 12.5, and

(a) curves at various pHs and the theoretical curve
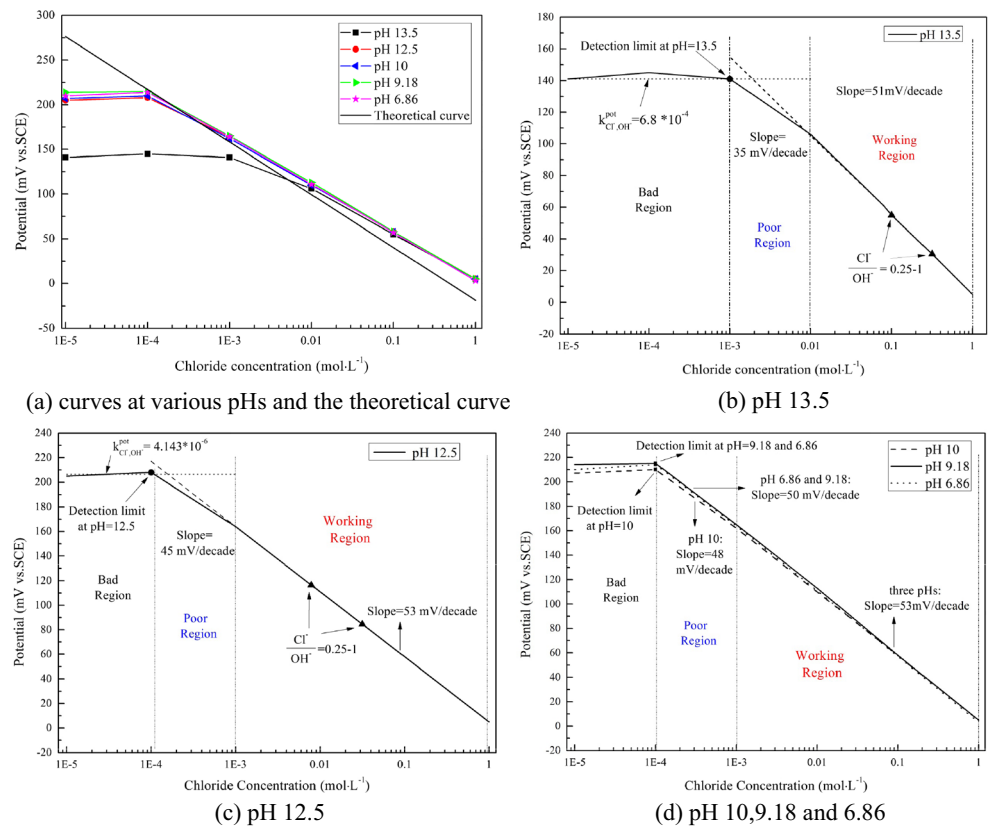
(b) pH 13.5

(c) pH 12.5

(d) pH 10, 9.18 and 6.86

Fig. 2d indicates the electrode potential against the chloride concentration at pH 10, 9.18 and 6.86.

Unlike pH 13.5, in these pH values, the working region is between 10^{-3} and 1 mol L^{-1} chloride concentration; meanwhile, the slope of these measured curves is ca. 53 mV/decade. It is necessary to point out that the slope is as low as 45 mV/decade in the poor region at pH 12.5, which is 10 mV lower than the slope in the working region. However, at pH 10, 9.18, and 6.86, the difference of the slope in the poor and working range is only 4 mV/decade, which indicates that the electrode potential still has a good sensitivity to the chloride concentration in the poor region. The reason is that the OH⁻

concentration is less than 10^{-4} mol L^{-1} when the pH is lower than 10; in this case, the OH⁻ has little interference on the sensitivity of electrode potential to the chloride concentration. Moreover, the electrode potential is no longer changed in the bad region as well.

When regard to chloride induced corrosion, the ratio of [Cl⁻]/[OH⁻] has been considered functional. The threshold value of Cl⁻/OH⁻ was determined in the simulated concrete pore solution ranges from 0.25 to 1. The pH value of concrete pore solution is usually 12.6, even up to 13.5 due to the fact that pore fluid consists of NaOH and KOH in addition to Ca(OH)₂ solution (pH 12.6). Figure 2b, c indicates that the

Table 2 Detection critical values and slopes of calibration curves at various pH values

Solution	chloride range(mol L^{-1})	Slope(mV/decade)	detection critical value(mol L^{-1})
pH 6.86	10^{-3}–10^{-0}	54	10^{-4}
	10^{-4}–10^{-3}	50	
pH 9.18	10^{-3}–10^{-0}	53	10^{-4}
	10^{-4}–10^{-3}	50	
pH 10.0	10^{-3}–10^{-0}	53	10^{-4}
	10^{-4}–10^{-3}	48	
pH 12.5	10^{-3}–10^{-0}	53	10^{-4}
	10^{-4}–10^{-3}	45	
pH 13.5	10^{-2}–10^{-0}	52	10^{-3}
	10^{-4}–10^{-2}	35	

chosen critical Cl⁻ to OH⁻ ratio of 0.25^{-1} is in the working region at pH 13.5 and 12.5. For this reason, the hydroxide interference is thus not significant at such chloride concentrations.

Sensitivity to sulfate ion Sulfate attack is one of the main reasons that can cause coastal structures to fail [28]. The sulfate penetration profile in concrete even can exceed the mass fraction of 2.846 % [29]. The electrode potential in solution containing 0.002 mol L⁻¹ sulfate ion concentration is only 2 mV difference with the electrode potential in 0.5 mol L⁻¹. What is more, the electrode potential keeps the same value when the sulfate ion concentration ranges from 0.01 to 0.5 mol L⁻¹. It can be clearly found that the sulfate ion concentration has little influence on the electrode potential. In other words, the electrode potential is not sensitive to the sulfuric acid activity. Based on this, the Ag/AgCl electrodes can be applied to monitor the chloride concentration in concrete pore solution even if the concrete has also suffered serious sulfate attack.

Effect of temperature The theoretical value at different temperatures can be calculated according to Eq. (1). These measured slopes and the theoretical ones are all presented in Table 3. In addition, the measured slopes are similar to the slopes reported by Montemor [3]. When the electrodes are used to monitor the chloride concentration, it is necessary to know the true temperature of the environment. The same potential presents different chloride contents in different temperatures. The chloride concentration based on the electrode potential can be more accurate if the interference of the temperature is eliminated.

Besides, the measured electrode potential can be written as follow:

$$E_m = E^o_{Ag/AgCl} - \frac{RT}{F}\ln[Cl^-] - E_{RE} \qquad (7)$$

When the Ag/AgCl electrode is used as electrode, the interference of $E^o_{Ag/AgCl}$ will be eliminated; thus, the temperature only affects RT/F [25]. But if the reference electrode is other type, accurate values for $E^o_{Ag/AgCl}$ and E_{RE} are necessary to be used, which can be found in these literatures [30,

Table 3 Theoretical slopes and measured slopes of electrodes at different temperatures

Temperature (°C)	Theoretical slope (mV/decade)	Experimental slope (mV/decade)
4	−55	−50
15	−57	−54
30	−60	−56
45	−63	−58

31]. It is well known that the saturated calomel electrode (SCE) is commonly used as reference electrode. It should be noted that the Ag/AgCl electrode and the SCE have similar temperature coefficients of ca. −0.6 to −0.65 mV °C⁻¹ [25]. Based on this, the error is quite small when the complete measurement according to Eq. (7) is considered. So it is recommended to use the SCE as the reference electrode to measure the potential of Ag/AgCl electrode.

Polarization tests

Potentiodynamic polarization tests Results of the potentiodyamic polarization tests are shown in Fig. 3 for the Ag/AgCl electrodes. Duplicate experiments provided essentially the same results. The exchange current density characterizes the capacity of polarization resistance, which can be fitted from the potentiodynamic polarization curves. The exchange current density can be calculated from Eq. (8):

$$I_o = \frac{RT}{F}\frac{\delta I}{\delta U} \qquad (8)$$

According to Kelly [32] and JIN [23], the acceptable high exchange current density is 30 μA/cm². Potentiodynamic polarization tests of Ag/AgCl electrodes in solutions A–E without chloride are shown in Fig. 3a. The anodic currents remained relatively low above the corrosion potential at pH <13, which are lower than 10⁻² μA/cm². Nevertheless, the anodic current exceeds 0.1 μA/cm² at pH 13.5. The exchange current densities of Ag/AgCl electrodes in concrete environments derived from the potentiodynamic polarization curves are given in Table 4a. The exchange current densities of the electrodes in simulated concrete pore solutions at different pH values all exceed 30 μA/cm², which proves that the electrode has good ability of resisting polarization. Here, it was found that the exchange current density reached maximum at pH 12.5. What is more, at pH 13.5 and pH 10, an obvious anodic peak was found at low overpotentials. The anodic peak is probably due to the formation of some silver oxides [33]. Potentiodynamic polarization tests of Ag/AgCl electrodes in solution A with different chloride contents are shown in Fig. 3b. The anodic peak appeared in every curve. Most of anodic currents in different chloride concentrations lay between 0.1 and 1 μA/cm². The exchange current densities of Ag/AgCl electrode in different chloride concentrations derived from the potentiodynamic polarization curves are given in Table 4b. It is clearly found that the exchange current density becomes larger with the chloride concentration increasing.

EIS tests The Nyquist diagrams for Ag/AgCl electrode in solutions are shown in Fig. 4. According to literature [34], the equivalent-circuit model which is applied to analyze the

(a) at various pHs
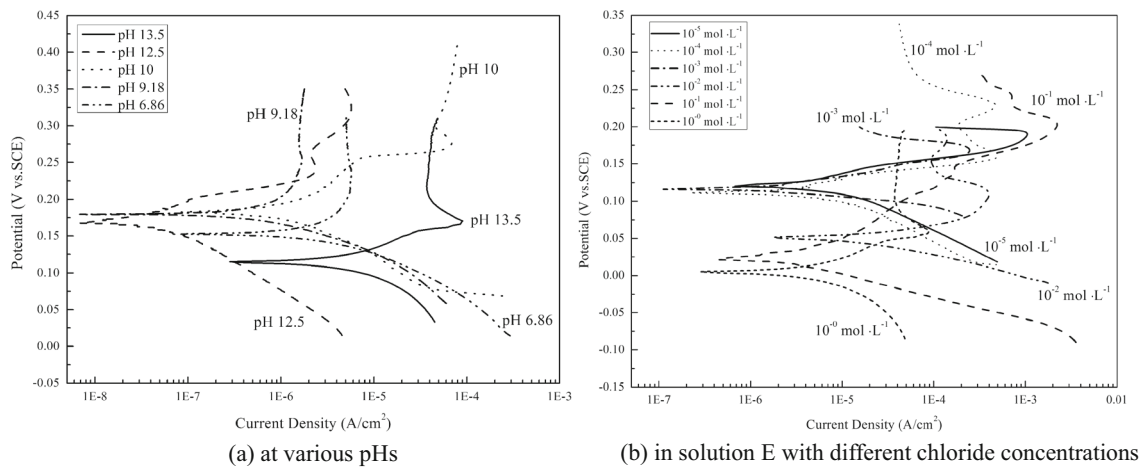(b) in solution E with different chloride concentrations

Fig. 3 Potentiodynamic polarization curves of Ag/AgCl electrodes in silulated concrete solutions

EIS is shown in Fig. 5. The equivalent-circuit model consists of a constant phase-angle element (CPE) in parallel with the polarization resistance (R_p) in addition to the electrolyte resistance (R_e). In this model, a CPE is used instead of a capacitance to account for the non-ideal capacitive response. Furthermore, the CPE is characterized by an admittance coefficient (Yo) and a frequency exponent n. The parameters are used to compute the apparent capacitance [35]. Figure 4a indicates the Nyquist diagrams for Ag/AgCl electrodes in solutions A–E. The apparent capacitance and frequency exponent n of Ag/AgCl electrodes derived from Fig. 4a are listed in Table 5a. The capacitance values at pH 6.86–12.5 only changed from 0.9 to 1×10^{-4} F cm^{-2}, which is independent of the pH value. But it should be noted that the capacitance value at pH 13.5 is several times larger than the ones at other pH values. The Nyquist diagrams of electrodes in solution A with different chloride contents are shown in Fig. 4b. The apparent capacitance and frequency exponent n derived form Fig. 4b are also given in Table 5b. The apparent capacitances in different chloride concentrations are between 3.5 and 5.4×10^{-4} F cm^{-2}, which proves that the chloride concentration in solution has little influence on the capacitance value of electrode. Moreover, the capacitance of Ag/AgCl electrode is more than one order larger than the capacitance value of MnO$_2$ reference electrode [36]. It was found that Ag/AgCl electrode shows high equivalent capacitance, which implies low electrode impedance. And this capacitive behavior provides tolerance to brief current incursions. Actually, it will inevitably lead to a small current to pass the Ag/AgCl electrode when embedding them in concrete structure to monitor the chloride concentrations. But the Ag/AgCl electrode has the ability to pass brief small currents with a minimum of polarization when conducting electrochemical measurements in concrete structure.

Galvanostatic tests The Ag/AgCl electrodes were tested in SCS with 0, 0.1, and 1 mol L^{-1} chloride concentration. After a quasi-stabilization period of 3 days, a cathodic direct current of 0.05 μA was applied for a period of 100 h. Then, the potential was tested for another period of 3 days. Results of the galvanostatic tests in solutions with different chloride concentrations are shown in Fig. 6. The electrode potential stabilizes quickly in solutions containing chloride; nevertheless, it took several hours to get the equilibrium potential in solutions without chloride.

It is clearly seen from Fig. 6 that the electrode shows little hysteresis and a little shift in potential when a cathodic current is applied. Besides, it recovers almost instantaneous after the interruption of the current. What is more, the polarization resistances of Ag/AgCl electrodes in SCS containing 0, 0.1, and 1 mol L^{-1} chloride content are 100, 10, and 225 kΩ, respectively. Thus, the potential shifts only 0.5 mV in SCS

Table 4 Exchange current density for Ag/AgCl electrode in simulated concrete solutions

(a) At various pHs					
	pH 6.86	pH 9.18	pH 10	pH 12.5	pH 13.5
I_o (μA/cm^2)	35	45	40	70	60
(b) In solution E with different chloride contents					
	10^{-0} mol L^{-1}	10^{-1} mol L^{-1}	10^{-2} mol L^{-1}	10^{-3} mol L^{-1}	10^{-4} mol L^{-1}	10^{-5} mol L^{-1}
I_o (μA/cm^2)	80	88	75	61	65	62

(a) at various pHs
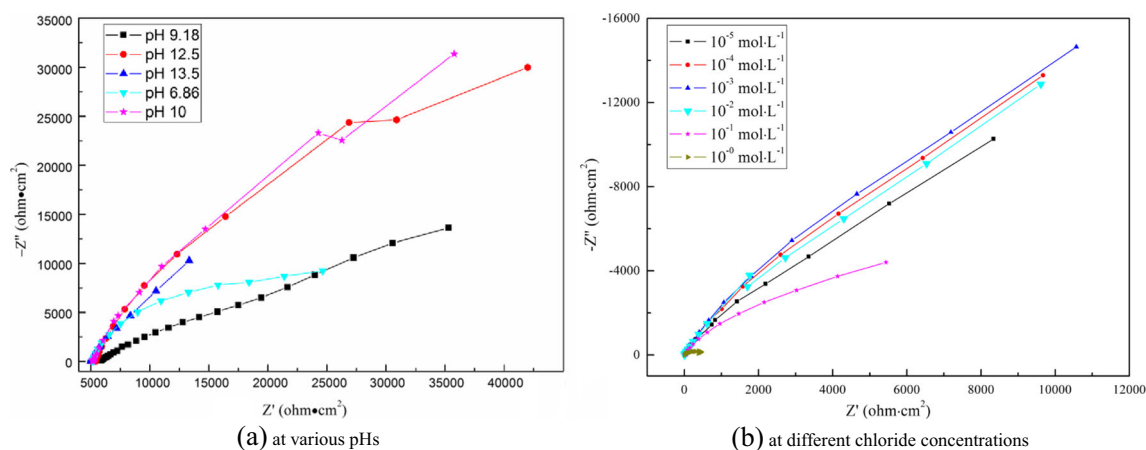
(b) at different chloride concentrations

Fig. 4 Nyquist diagrams for Ag/AgCl electrode in simulated concrete solutions

with 0.1 mol L^{-1} chloride concentration, which is almost negligible. Moreover, the potential shifts 5 and 11 mV in SCS with 0 and 1 mol L^{-1} chloride concentration, respectively. It should be pointed out that the cathodic current density we applied in the galvanostatic tests was as high as 0.8 μA/cm². But the measured potential change of electrodes in SCS was less than 12 mV. However, for a typical input bias current of 1 nA, potential shifts lower than 0.225 mV are obtained. So it is concluded that the Ag/AgCl electrode resists the long-term effect of the application of small bias currents commonly found in electrochemical instruments.

Long-term stability

Figure 7 shows the potentials of the Ag/AgCl electrodes immersed in solutions of various pH values containing different chloride concentrations versus time as described in "Long-term stability." In the presence of chloride, the potentials stabilize quickly and kept the stable state over the complete exposure time. Even after 3 months immersion, the electrode potentials are still consistent with those measured in the calibration tests (Fig. 2a). The same results are reported by Angst et al. [25]. However, in the absence of chloride, the potentials appear to be dependent on pH value, being generally lower with increasing solution alkalinity. Meanwhile, they are less stable compared with those in the chloride containing

Fig. 5 Equivalent-circuit model applied to analyze the EIS results for the Ag/AgCl electrodes in simulated concrete solutions

solutions and decrease monotonously over time. However, this is most pronounced during the first 20 days, the values are more stable in the subsequent testing time. Kalcher [37] reported that Ag/AgCl electrodes in chloride-free, alkaline sodium hydroxide solutions showed lower potentials when the pH was above 12, and approached the value of $E^o_{Ag/Ag2O}$ at pH 14. It can be clearly seen from Fig. 7 that eventually the final potentials are close to $E_{Ag/Ag2O}$ at pH 12.5 and 13.5, thereby implying that the electrode coating is continuously transformed into Ag_2O and thus the electrode acts as a pH sensor rather than a chloride sensor. However, at pH 9.18, it can be clearly found that the electrode potential is lower than the value of corresponding $E_{Ag/Ag2O}$. The reason is that little AgCl coating has transformed into Ag_2O at pH 9.18.

In order to study the uncertainties with regard to chemical transformation of AgCl at high pH values, microanalysis of electrodes was carried out. Figure 8 indicates the scanning electron micrographs of AgCl electrodes after more than 3 months of constant immersion. It can be obviously found that the surface morphology of electrode exposed to low alkaline (pH 9.18), even in the absence of chloride ions (Fig. 8c), is similar to the ones immersed in a highly alkaline (pH 13.5), but chloride containing solution (Fig. 8b). The AgCl coating adhered to the Ag probe is very dense and has few detects. Figure 8d is the micrograph of electrode exposed to moderately alkaline (pH 12.5) without chloride in which the hydroxide ions concentration was ca. 0.0316 mol L^{-1}. The most area of the AgCl coating was still dense but some small cracks and tiny holes appeared in the coating. In the case of pH 13.5 and in the absence of chloride, on the other hand, the electrode coating exhibits a clearly rough surface topography (Fig. 8a). The coating is no longer dense and it becomes loose and porous after immersion. The explanation is that the AgCl coating had been transformed into the Ag_2O, which results in generating a lot of defects on the surface.

The existence of Ag_2O on the electrode coating can be verified by examining the coating through the energy-
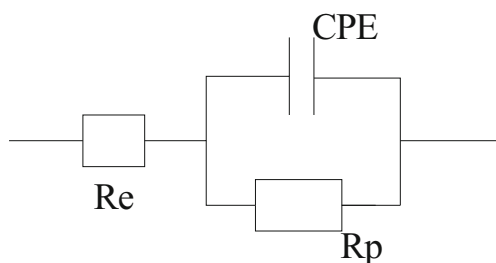
Table 5 The apparent capacitance and frequency exponent n of Ag/AgCl electrodes obtained from EIS measurements

(a) At various pHs

	pH 6.86	pH 9.18	pH 10	pH 12.5	pH 13.5	
Apparent Capacitance(F/cm^2)	9.067×10^{-5}	5.033×10^{-5}	1.181×10^{-4}	1.067×10^{-4}	4.918×10^{-4}	
Frequency Exponent n	0.8	0.8	0.8	0.8	0.8	

(b) In solution E with different chloride contents

	10^{-0} mol L^{-1}	10^{-1} mol L^{-1} L^{-1}	10^{-2} mol L^{-1} mol	10^{-3} mol L^{-1}	10^{-4} mol L^{-1}	10^{-5} mol L^{-1}
Apparent Capacitance(F/cm^2)	4.998×10^{-4}	4.127×10^{-4}	3.639×10^{-4}	3.588×10^{-4}	5.152×10^{-4}	5.344×10^{-4}
Frequency Exponent n	0.8	0.8	0.8	0.8	0.8	0.8

dispersive spectrometry (EDS). In the case of pH 13.5 and in the absence of chloride, the EDS of the electrode coating is shown in Fig. 9a. It can be clearly found that the coating is made up of Ag_2O, in which there was almost no AgCl. But at the case of pH 13.5 with 0.1 mol L^{-1} chloride concentration (Fig. 9d), there is no Ag_2O in the coating of electrode. Only the AgCl is detected in the coating. In addition, Fig. 9d is similar with Fig. 9c. However, in the case of pH 12.5 and absence of chloride, the EDS of the electrode coating (Fig. 9b) proves that the AgCl and Ag_2O coexist in the coating together.

The EDS of electrode coating is consistent with the micrograph of electrodes surface. At the case of pH 12.5 without chloride, the EDS shows AgCl and Ag_2O coexist in the electrode coating, which leads to some small defects in the surface (Fig. 8d). Figure 9c, d indicates that the coating is fully made up of AgCl; therefore, the coating is dense as shown in Fig. 8b, c. In the case of pH 13.5 and absence of chloride, the membrane consists of Ag_2O and little AgCl; thus, the

coating is loose and porous. In a word, the EDS of electrodes coincides well with the micrograph.

Tests in concrete

After curing for 3 weeks, the concrete compressive strength was ca. 27 MPa. Figure 10 shows the chloride electrode potential as a function of time about 1 year, when exposed to different chloride solutions. Initially, the electrodes in all specimens show high values (ca. 210 mV vs. SCE), but the electrode potentials drop rapidly after immersion in chloride contained solutions. After ca. 150 days, the electrodes show approximately steady values. However, the electrodes in specimens immersed in distilled water stabilize after 100 days and the decreased potential is only 20 mV. The electrode potentials are analyzed statistically after they get stable. The actual chloride concentrations of concrete pore solutions (actual value), the chloride concentrations calculated by the electrode potentials (calculated value), and the differences are all listed in Table 6. The concentrations obtained from the embedded electrodes are in good agreement with the chloride concentrations
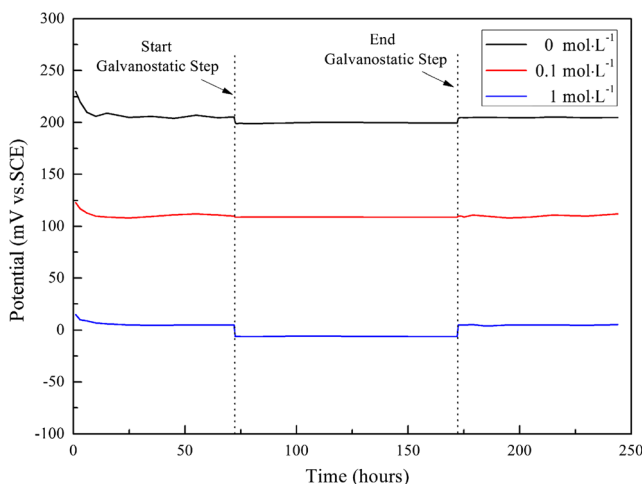

Fig. 6 Potential of Ag/AgCl electrode in SCS with different chloride concentrations. *Vertical dotted lines* indicate the start and end of the galvanostatic pulse
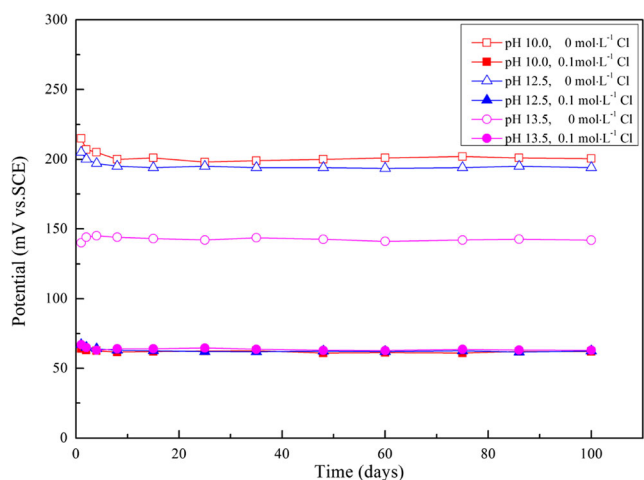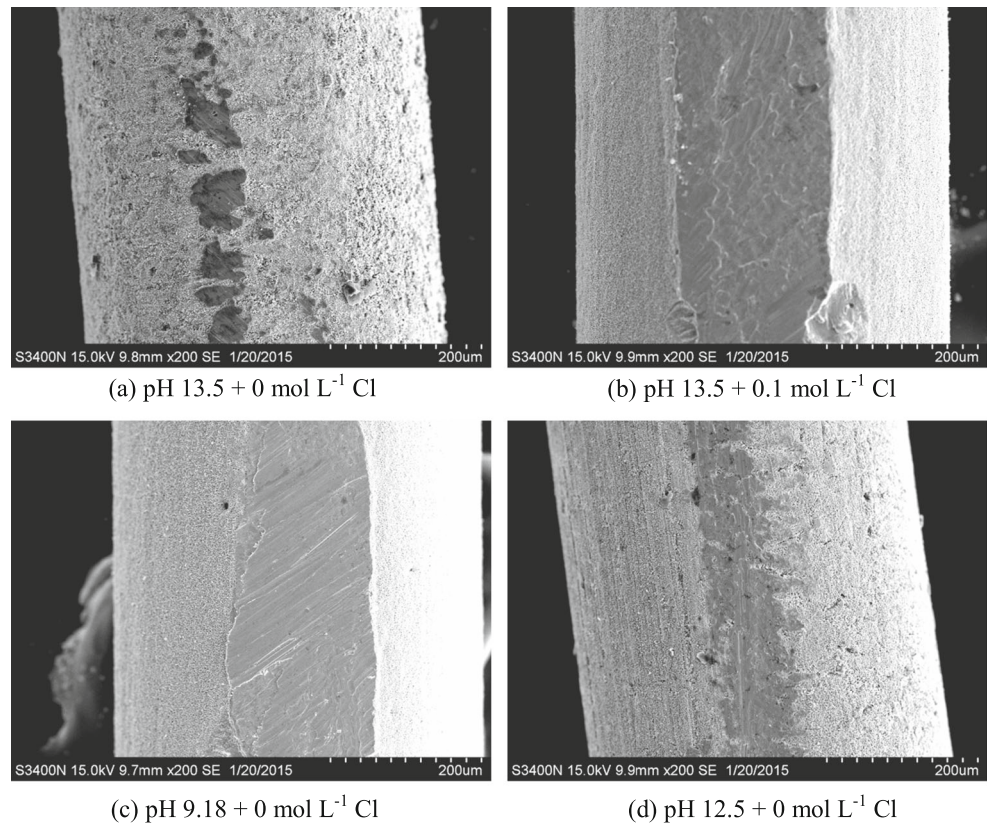

Fig. 7 Potential of Ag/AgCl electrode in solutions of various pHs and chloride concentrations versus time
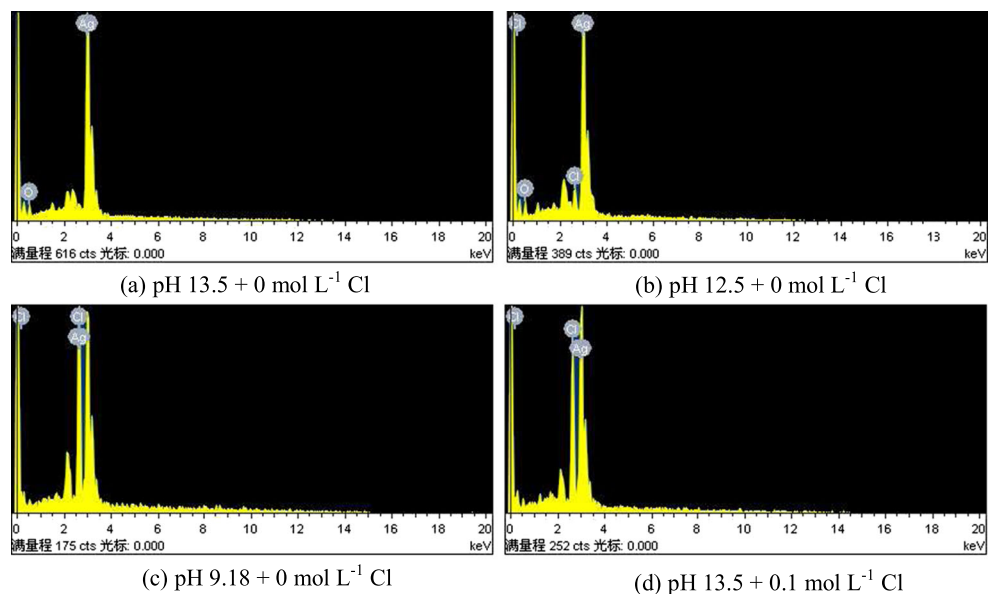
Fig. 8 SEM micrographs of the Ag/AgCl electrode membranes after more than 3 months immersion in solutions with various pHs and chloride concentrations

(a) pH 13.5 + 0 mol L^{-1} Cl

(b) pH 13.5 + 0.1 mol L^{-1} Cl

(c) pH 9.18 + 0 mol L^{-1} Cl

(d) pH 12.5 + 0 mol L^{-1} Cl

measured in the expressed concrete pore solutions. But it should be noted that there is an obvious difference between the value calculated by the electrode potentials and the value determined in the concrete pore solutions. This difference is found to be negative, and the difference seems to be larger with the increase of chloride concentration in solution. This difference is probably due to the potential error of electrode potential compared with the SCE placed on the external solution of concrete, which can be attributed to the diffusion potential [38], liquid junction potential, and membrane potential [38, 39]. This potential error can be diminished through embedding the reference electrode in the concrete, and further, the reference electrode should be placed close to the working electrode as much as possible.

Fig. 9 Energy-despersive spectrometry (EDS) of Ag/AgCl electrode coating after more than 3 months immersion in solutions with various pHs and chloride concentrations
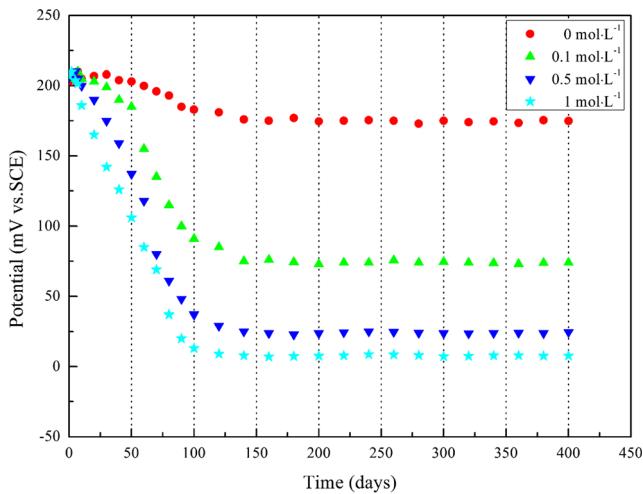

(a) pH 13.5 + 0 mol L^{-1} Cl

(b) pH 12.5 + 0 mol L^{-1} Cl

(c) pH 9.18 + 0 mol L^{-1} Cl

(d) pH 13.5 + 0.1 mol L^{-1} Cl

Fig. 10 Potential of the chloride electrodes embedded in concrete vs time of immersion in solutions with different chloride concentrations

Additional remarks on the use of ISE in concrete

It was clearly shown above that the high pH value of solution can affect the Ag/AgCl electrode potential, especially in the absence of chloride. The former AgCl coating will transform into Ag_2O if the electrodes are immersed in high alkaline solutions without chloride during a long time. However, the electrodes recover fast as soon as they come into contact with chloride, which is also reported in the literature [25]. Furthermore, the eventual formation of silver oxide is fully reversible. Actually, many researches [2, 3, 17, 19, 24, 40] have embedded the Ag/AgCl electrodes in mortar or concrete to monitor the free chloride concentrations in concrete pore solutions. They reported that it was credible to obtain the chloride concentrations in concrete structures based on the date provided by the electrodes. What is more, the electrode exhibits good state for a long time.

From an engineering point of view, it is useful and necessary to predict the front of the chloride invasion. The traditional methods such as extracting concrete pore solution are really heavy and destructive. Hence, it is convenient to detect the front of chloride invasion by embedding the electrodes in concrete.

Conclusions

From the present experimental investigation, following conclusions can be drawn:

(1) Ag/AgCl electrodes can be successfully used to measure the chloride concentration in concrete. The detection limit for chloride ion is 10^{-3} mol L^{-1} at pH 13.5 and 10^{-4} mol L^{-1} at lower values. In addition, the detecting region in different chloride contents can be divided into working, poor, and bad region, respectively. In addition, the threshold values of Cl^-/OH^- (0.25^{-1}) in high alkaline solutions are all located in working region.

(2) The Ag/AgCl electrode potential is not affected by the sulfate ion concentration. Moreover, it is necessary to acquire the accurate temperature of the electrode for the reason that the same potential presents different chloride concentrations in different temperatures. And the SCE is recommended to work as the reference electrode because the SCE has the similar temperature coefficient with the Ag/AgCl electrode.

(3) The exchange current density of Ag/AgCl electrode in simulated concrete solution exceeds 30 $\mu A/cm^2$. And the electrode also shows a high equivalent capacitance. Both of them indicate that the electrode has good ability on resisting polarization. Furthermore, the potential change of electrode in saturated $Ca(OH)_2$ solution is less than 12 mV even if the applied current density is as high as 0.8 $\mu A/cm^2$. Based on this, the electrodes can resist the long-term effect of the application of small bias currents commonly found in electrochemical instruments.

(4) The AgCl coating shows good long-term stability during immersion in simulated concrete pore solutions. Some of AgCl coating will transform into Ag_2O when the electrodes are immersed in high alkaline solutions without chloride. Nevertheless, the formation of Ag_2O is fully reversible when the electrode is placed in solutions with chloride.

(5) The chloride concentration calculated by the embedded electrodes in concrete has good agreement with the value determined by the expressed concrete pore solution. Besides, the electrode potential error can be reduced by placing the reference electrode near the working electrode as much as possible.

Table 6 Chloride contents measured in different experiments in the external solution, in the expressed pore solution compared to the content calculated from the chloride electrode potential

Chloride solution(mol L^{-1})	Actual content (mol L^{-1})	Calculated content (mol L^{-1})	Standard deviation (mol L^{-1})
0.1	0.08	0.05	−0.03
0.5	0.47	0.44	−0.04
1.0	0.90	0.83	−0.07

References

1. Xu J, Jiang L, Wang W, Tang L, Cui L (2013) Effectiveness of inhibitors in increasing chloride threshold value for steel corrosion. Water Sci Eng 6(3):354–363

2. Elsener B, Zimmermann L, Böhni H (2003) Non destructive determination of the free chloride content in cement based materials. Mater Corros 54(6):440–446

3. Montemor MF, Alves JH, Sim Es AM, Fernandes JCS, Louren OZ, Costa AJS, et al (2006) Multiprobe chloride sensor for in situ monitoring of reinforced concrete structures. Cem Concr Compos 28(3):233–236

4. Xu J, Jiang L, Wang W, Jiang Y (2011) Influence of CaCl2 and NaCl from different sources on chloride threshold value for the corrosion of steel reinforcement in concrete. Constr Build Mater 25(2):663–669

5. Xu J, Jiang L, Wang J (2009) Influence of detection methods on chloride threshold value for the corrosion of steel reinforcement. Constr Build Mater 23(5):1902–1908

6. Ann KY, Song H (2006) Chloride threshold level for corrosion of steel in concrete. Corros Sci 49(11):4113–4133

7. Torres-Luque M, Bastidas-Arteaga E, Schoefs F, Sánchez-Silva M, Osma JF (2014) Non-destructive methods for measuring chloride ingress into concrete: state-of-the-art and future challenges. Constr Build Mater 68:68–81

8. Oh BH, Jang SY (2007) Effects of material and environmental parameters on chloride penetration profiles in concrete structures. Cem Concr Res 37(1):47–53

9. Sanchez-Silva M, Klutke G, Rosowsky DV (2011) Life-cycle performance of structures subject to multiple deterioration mechanisms. Struct Saf 33(3):206–217

10. Alonso MC, Sanchez M (2009) Analysis of the variability of chloride threshold values in the literature. Mater Corros 60(8):631–637

11. Garzon AJ, Sanchez J, Andrade C, Rebolledo N, Menéndez E, Fullea J (2013) Modification of four point method to measure the concrete electrical resistivity in presence of reinforcing bars. Cem Concr Composs 53:249–257

12. Taillet E, Lataste JF, Rivard P, Denis A (2014) Non-destructive evaluation of cracks in massive concrete using normal dc resistivity logging. NDT& E INT 63:11–20

13. Morris W, Moreno EI, Sagues AA (1996) Practical evaluation of resistivity of concrete in test cylinders using a Wenner array probe. Cem Concr Res 26(12):1779–1787

14. Nguyen TH, Venugopala T, Chen S, Sun T, Grattan KTV, Taylor SE, et al (2014) Fluorescence based fibre optic pH sensor for the pH 10–13 range suitable for corrosion monitoring in concrete structures. Sensors Actuators B: Chem 191:498–507

15. Maaskant R, Alavie T, Measures RM, Tadros G, Rizkalla SH, Guha-Thakurta A (1997) Fiber-optic Bragg grating sensors for bridge monitoring. Cem Concr Compos 19(1):21–33

16. Davis MA, Bellemore DG, Kersey AD (1997) Distributed fiber Bragg grating strain sensing in reinforced concrete structural components. Cem Concr Compos 19(1):45–57

17. Climent-Llorca MA, Viqueira-Pérez E, López-Atalaya MM (1996) Embeddable Ag/AgCl sensors for in-situ monitoring chloride contents in concrete. Cem Concr Res 26(8):1157–1161

18. Atkins CP, Carter MA, Scantlebury JD (2001) Sources of error in using silver/silver chloride electrodes to monitor chloride activity in concrete. Cem Concr Res 31(8):1207–1211

19. Duffo GS, Farina SB (2009) Development of an embeddable sensor to monitor the corrosion process of new and existing reinforced concrete structures. Constr Build Mater 23(8):2746–2751

20. McCarter WJ, Vennesland Ø (2004) Sensor systems for use in reinforced concrete structures. Constr Build Mater 18(6):351–358

21. Li H, Li D, Song G (2004) Recent applications of fiber optic sensors to health monitoring in civil engineering. Eng Struct 26(11):1647–1657

22. Umezawa Y (1990) CRC handbook of ion-selective electrodes: selectivity coefficients: CRC press Boca Raton, FL

23. Jin M, Xu J, Jiang L, Gao G, Chu H, Xiong C, et al (2014) Electrochemical characterization of a solid embeddable Ag/AgCl reference electrode for corrosion monitoring in reinforced concrete. Electrochemistry 82(12):1040–1046

24. Atkins CP, Scantlebury JD, Nedwell PJ, Blatch SP (1996) Monitoring chloride concentrations in hardened cement pastes using ion selective electrodes. Cem Concr Res 26(2):319–324

25. Angst U, Elsener B, Larsen CK, Vennesland Ø (2010) Potentiometric determination of the chloride ion activity in cement based materials. J Appl Electrochem 40(3):561–573

26. Janata J (1989) Principles of chemical sensors. Plenum Press, New York

27. Koryta J (1972) Theory and applications of ion-selective electrodes. Anal Chem Acta 61(3):329–411

28. Sun C, Chen J, Zhu J, Zhang M, Ye J (2013) A new diffusion model of sulfate ions in concrete. Constr Build Mater 39:39–45

29. Tumidajski PJ, Chan GW, Philipose KE (1995) An effective diffusivity for sulfate transport into concrete. Cem Concr Res 25(6):1159–1163

30. Ives DJ, Janz GJ, King CV (1961) Reference electrodes: theory and practice. J Electrochem Soc 108(11):246–247

31. Dobos D (1975) Electrochemical data: a handbook for electrochemists in industry and universities. Elsevier Scientific Publishing Company Amsterdam

32. Brossia CS, Kelly RG (1996) A reference electrode for use in methanol solutions. Electrochim Acta 41(16):2579–2585

33. Teijelo ML, Vilche JR, Arvia AJ (1984) The electroformation and electroreduction of anodic films formed on silver in 0.1 < i > M sodium hydroxide in the potential range of the Ag/Ag < sub > 2 O couple. J Electroanal Chem Interfacial Electrochem 162(1):207–224

34. Duffó GS, Farina SB, Giordano CM (2009) Characterization of solid embeddable reference electrodes for corrosion monitoring in reinforced concrete structures. Electrochim Acta 54(3):1010–1020

35. Hsu CH, Mansfeld F (2001) Technical note: concerning the conversion of the constant phase element parameter Y0 into a capacitance. Corrosion 57(9):747–748

36. Muralidharan S, Saraswathy V, Thangavel K, Palaniswamy N (2008) Electrochemical studies on the performance characteristics of alkaline solid embeddable sensor for concrete environments. Sensors Actuators B: Chem 130(2):864–870

37. Svegl F, Kalcher K, Grosse-Eschedor YJ, Balonis M, Bobrowski A (2006) Detection of chlorides in pore water of cement based materials by potentiometric sensors. Rare Metal Mater Eng 35:232–237

38. Angst U, Vennesland Ø (2009) Detecting critical chloride content in concrete using embedded ion selective electrodes—effect of liquid junction and membrane potentials. Mater Corros 60(8):638–643

39. Angst U, Vennesland Ø, Myrdal R (2009) Diffusion potentials as source of error in electrochemical measurements in concrete. Mater Struct 42(3):365–375

40. Angst UM, Polder R (2014) Spatial variability of chloride in concrete within homogeneously exposed areas. Cem Concr Res 56:40–51